# Electrochromism of NiO-$TiO_2$ sol gel layers

**A. Al-Kahlout · S. Heusing · M. A. Aegerter**

**Abstract** Films of NiO-$TiO_2$ with Ni concentration of 100, 90, 87, 83, 75, 66, 50 and 33 mol% have been obtained via the sol-gel route by dip coating technique and sintered in air between 250 and 500°C using ethanolic sols of nickel acetate tetrahydrate ($Ni(CH_3COO)_2{\cdot}4H_2O$) and titanium *n*-propoxide ($Ti(O\text{-}CH(CH_3)_2)_4$) precursors. Xerogels obtained by drying the sols have been studied up to 900°C by thermal analysis (DTA/TG) coupled to mass and IR spectroscopy. The crystalline structure and morphology of the layers in the as deposited, bleached and colored states were determined by X-ray diffractometry, scanning electron microscopy and transmission electron microscopy Their electrochromic properties have been studied in 1 M KOH aqueous electrolyte as a function of the layer composition, thickness and sintering temperature. Deep brown colour with reversible transmittance changes have been obtained using cycling voltammetry and chronoamperometry processes. The best composition to get stable sols, a high reversible transmittance change and fast switching times (<10 s) was obtained with double NiO-$TiO_2$ layers 160 nm thick having 75% Ni molar concentration, and sintered between 300 and 350°C. The mechanism of coloration and morphology transformation of the layer during cycling are discussed in terms of an activation and degradation period. The results are in agreement with the accepted Bode model.

**Keywords** Sol-gel · NiO-$TiO_2$, · Thin film · Dip-coating · Electrochromism · Thermal analysis

## 1. Introduction

Electrochromic materials are able to change reversibly their optical properties usually upon charge insertion and extraction induced by an external voltage [1, 2]. NiO is a transparent slightly greenish anodic electrochromic material which colors brown due to the oxidation of $Ni^{2+}$ to $Ni^{3+}$. It is an inexpensive material that has a rather high electrochromic efficiency [3]. It is therefore a promising material to be used in form of layers in battery type electrochromic (EC) devices. It can be used as a coloring anodic ion- storage film either with a passive cathodic EC layer (e.g. a $CeO_2$-$TiO_2$) or with a cathodic coloring EC materials (e.g. a $WO_3$ or $Nb_2O_5$ layers). In this last case it is possible to get an increase of the transmittance change because of the simultaneous coloration of the anodic and cathodic layers [4].

Electrochromic thin films of nickel oxide have been essentially produced by physical techniques, the most common ones being dc and rf reactive magnetron sputtering [5–7], pulsed laser deposition [8] and electron beam evaporation [9]. Because of the lack of suitable precursors which often have insufficient solubility and stability, only few works have been reported on the preparation of films by chemical methods such as anodic and cathodic electrodeposition [10, 11], chemical vapor deposition [12] and sol-gel [3, 13–24].

Sol-gel NiO films have been prepared using aqueous sols of nickel hydroxide $Ni(OH)_2$ obtained by precipitating $NiSO_4$ in presence of LiOH and acetic acid [13, 15, 16], or by alternate immersion in $NiSO_4$ and KOH solutions [3]. More recently alcoholic sols have been used such as sols of nickel diacetate tetrahydrate ($Ni(CH_3COO)_2{\cdot}4H_2O$) dissolved in either dry dimethylaminoethanol (dmaeth) [18] or in ethanol with additives [19], sols of nickel diacetate dmaeth ($Ni(acetate)_2(dmaeth)$) in dry dimethylaminoethanol [18], sols of nickel chloride ($NiCl_2$) dissolved with several

additives either in ethanol [19], or in 1-butanol [20] or in ethylene glycol [14]. Nickel nitrate hexahydrate ($Ni(NO_3)_2{\cdot}6H_2O$) dissolved in lower carbon alcohol with additives has been also used [19, 21]. One work reported the use of $Ni(OH)_2$ nanoparticles synthesized by precipitation of $NiCl_2{\cdot}H_2O$ [22]. It is also worthwhile to mention the preparation of Ni(Si)-oxide films where small NiO nanoparticles (size of 2,5 nm) have been grown at 300°C. The precursor was $Ni(OH)_2$ prepared from nickel sulphate heptahydrate in presence of LiOH [23]. Electrochromic lithiated nickel oxide ($Li_xNiO_2$, $0 \leq x \leq 1$) sintered at high temperature has been also reported [24].

After heat treatment at relatively low temperature $250 < T < 350$°C the sol-gel films phase structure observed by X-ray diffraction was always the bunsenite NiO form with a still important amorphous network. The crystallite size ranged from 10 nm [13] to about 150 nm [14] depending on the processing and sintering conditions.

The electrochromic properties of the sol-gel films have been mainly studied in KOH aqueous electrolyte and all presented a brown coloration with coloration efficiency measured at 550 nm ranging from 30 to 60 $cm^2/C$ depending on the processing and sintering conditions. The stability of the pure films in this electrolyte is poor.

In spite of the rich literature in the field of NiO electrodes, the mechanism of coloration is still not fully understood [2] but different processes have been proposed for NiO based films in aqueous electrolyte [8, 25–28] and in $Li^+$ based electrolyte [29]. It is nevertheless generally accepted that the reversible conversion from a bleached to a colored state is related to the redox process $Ni^{2+}/Ni^{3+}$ involving the transformation of $\beta$(II)-$Ni(OH)_2$ (transparent) into $\beta$(III)-NiOOH (colored) phases. However the exact identification and evolution of the different phases of the films during electrochemical cycling proposed in the so-called Bode scheme [30] (e.g the $\alpha$(II) and $\beta$(II)-$Ni(OH)_2$, $\beta$(III) and $\gamma$(III)-NiOOH) are by far not yet clear in spite of the thorough IR analysis by Orel's group [23].

Following ideas which led to the development of $CeO_2$-$TiO_2$ electrochromic sol-gel layers [31], for which it was found that very small $CeO_2$ crystallite nanoparticles can be grown in an amorphous $TiO_2$ matrix improving considerably the amount of charge that can be inserted reversibly into the electrode, the present study focuses on the preparation and characterization of NiO-$TiO_2$ films obtained by the dip coating process. Only two reports on the preparation of NiO-$TiO_2$ films have been published. They have been prepared with sol of $NiCl_2$ and Ti(iv)butoxide in 1-butanol [20], or by mixing nickel nitrate, nickel acetate or, nickel chloride and Ti(iv)alkoxide [19]. This paper presents a detailed study of the thermal behavior of xerogels, of the phase structure and morphology of the layers before and after coloration and of the electrochemical and optical behavior of layers tested in KOH electrolyte. A model based on these results to explain the mechanism of coloration and the film morphology transformation during cycling is proposed and discussed. The important result of this work is the experimental confirmation that the coloration of the layers during the initial cycles occurs in a very thin layer of about 50 nm at the interface electrolyte/coating (activation period) that grows with cycling till reaching the full thickness of the layer (steady state). Then a degradation period is observed in which the optical and electrochemical properties are gradually degradated, the layers becoming very soft and fragile to be even slowly detached from their support until the complete removal of the coating.

## 2. Experimental

An 0.5 M solution was prepared by dissolving $Ni(CH_3COO)_2{\cdot}4H_2O$ in ethanol at room temperature with continuous stirring for 7 h. Different amounts of titanium *n*-propoxide were dissolved in ethanol and then added to the Ni solution in a glove box filled with nitrogen (humidity RH $\leq$ 5%) to obtain Ni molar concentration varying between 100 to 33 mol%. The sols were then stirred at room temperature for 30 min. and finally filtered using a 0.2 $\mu$m Teflon filter.

Simultaneous Differential Thermal Analysis (DTA) and Thermogravimetry (TG) have been performed on xerogels dried overnight (Ni concentration 75 mol%) using a Netzsch STA 449C/3G Jupiter equipment coupled to Mass (MS) (QMS 403C Aeolos) and Infrared spectroscopy (IR) (Tensor 27-FTIR, Brucker). The xerogels were grounded in a mortar to get a fine powder. 33,3 mg of the powder was heated in synthetic air in an $Al_2O_3$ crucible up to 600°C at a heating rate of 2 K/min.

NiO-$TiO_2$ layers were deposited by the dip coating process (withdrawal speed of 3 mm/s, 20°C, RH = 40%) onto $10 \times 10\ cm^2$ float glass and commercial conducting $SnO_2$:F coated glass having a sheet resistance of 17 Ω/□ (K-glass). Up to 3 layers have been deposited. For this purpose a heat treatment in air was performed after each deposition at a rate of 2 K/min up to the desired temperature and then leaving the system at this temperature for about 30 min. Also single layers having different thicknesses have been deposited by changing the withdrawing speed from 0.5 to 4 mm/s. The thickness of the layers was determined by scratching the layer after drying and measuring the step height using a TENCOR P-10 surface profilometer.

The structural investigation of fresh triple layers deposited on float glass and heat treated from 250 to 500°C was achieved using X-ray difraction (XRD) (X'Pert Philips-MPD, Cu$K\alpha_{1,2}$) in the range $26° < 2\theta < 80°$ at 0.3° grazing incidence and scan steps of 0.02°. The crystallite size has been determined using the Scherrer equation. To test a possible change of the structure during the EC process,

triple layers have been also deposited onto 4 × 10 $cm^2$ ITO coated glass substrate (Asahi Glass). The NiO-$TiO_2$ layers have been cycled in 1 M KOH electrolyte during up to 270 voltametry (CV) cycles (see below), then disconnected at the positive potential (colored state + 1 V), or at the negative potential (bleached state −0.6 V) and dried in air before performing the XRD (range $10^\circ < 2\theta < 90^\circ$, 0.02° steps). The colored layers remained deeply coloured within the X-ray scan time of 12 h. For comparison, fresh layers have been also measured in the same way. Scanning Electron Microscopy (SEM) of the surface has been obtained using a JEOL JSM-6400F equipment, and Transmission Electron Microscopy (TEM) of fresh, bleached and colored thin rasped layers using a JEOL.JEM-2010 Gatan MSC equipment.

Electrochemical and in-situ optical measurements have been carried out using a three electrode cell (working electrode: NiO-$TiO_2$ layer deposited on *K*-glass, counter electrode: Platinum, reference electrode: SCE, electrolyte: 1 M KOH). Cyclic voltammetry (CV) and chronoamperometry (CA) measurements have been carried out using an EG&G 237A Potentiostat and transmittance measurements using a Carry 5E UV/VIS/NIR spectrometer. The experimental conditions are described later in the text.

## 3. Results and discussion

### 3.1. DTA/TG/MS/IR

The DTA/TG/DTG/GS spectra obtained for a NiO-$TiO_2$ xerogel (Ni concentration 75 mol%) are shown in Fig. 1. The Gram-Schmidt (GS) orthogonalization, a powerful data analysis tool [32], has been used to detect the presence of infrared radiation absorbing species evolved in the real time between 400 and 4000 $cm^{-1}$. The curve has an overall behavior similar to the DTA/DTG curves indicating that most of the species evolved in the temperature range are IR active. A first broad and small endothermic peak is observed at temperature below 200°C accompanied by a broad mass loss of about 10 wt% with a maximum slope (DTG) located at 90°C. This corresponds to the final drying of the xerogel as simultaneous MS (Fig. 2) and IR spectroscopy (Fig. 3), measured at 90°C show essentially the evolution of $H_2O$ (M/Z = 18, IR bands manifold around 1600 and 3700 $cm^{-1}$) with a small evolution of $CO_2$ (peaks at 650 and 2300 $cm^{-1}$) and alcohol (peaks at 1050 and 2900 $cm^{-1}$). Then a small exothermic DTA shoulder accompanied by a mass loss of 10 wt% occurs at about 240°C. The main fragments evolved observed by MS are $CO^+$ (CO, $CO_2$), $C_2H_4{}^+$($C_2H_4$) (M/Z = 28) and $O_2{}^+$ (O) (M/Z = 32) and by IR spectroscopy $CO_2$, alcohol and acetic acid (peaks at 600, 1000, 1200, 1400, 1800, 3000 and 3600 $cm^{-1}$). The main feature of the DTA curve is a strong exothermic double peak between 300 and 360°C with maximum at 344 and 357°C. These features are accompanied by a large two peaks mass loss of about 35 wt% with maximum at 340 and 352°C i.e. at about the same position as the DTA peaks (Fig. 1). A careful analysis of the infrared spectra of the gases evolved at these temperature (Fig. 3) shows that the organic compounds, acetic acid (or fragments) are essentially found during the first DTA peak (maximum at 344°C) but not during the sharp second DTA peak (max at 357°C). This is a strong indication that the formation of inorganic nickel compounds involving primarily $NiO_x$ and possibly $NiCO_3$ only occurs up to about 350°C The formation of $Ni(OH)_2$ is discarded as according to [33], this compound is already transformed into $NiO_x$ at 250°C. The last DTA peak, where mainly $CO_2$ and small amount of $H_2O$ are evolved, may possible be related to the transformation of $NiCO_3$ into NiO according to $NiCO_3 \rightarrow NiO + CO_2$ as suggested in [34].

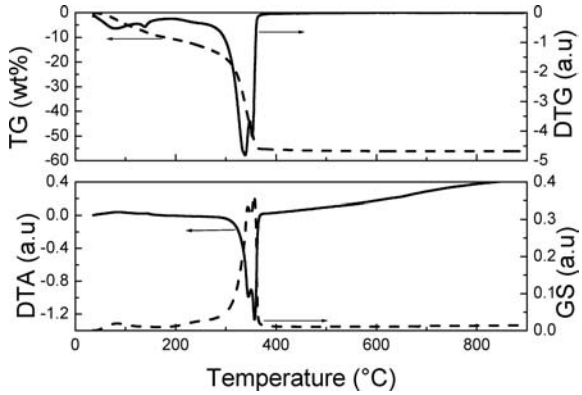


**Fig. 1** DTA/GS/TG/DTG thermal analysis of a xerogel (Ni content 75 mol%), heating rate 2 K/min in synthetic air. Top TG/DTG, bottom DTA/GS

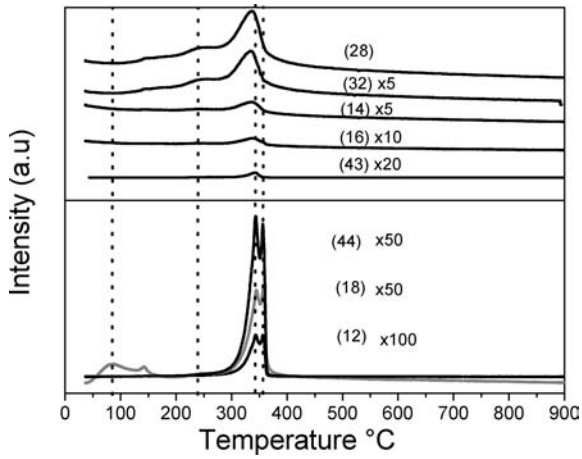


**Fig. 2** Selected mass spectra measured simultaneously during the DTA/TG measurements of a NiO-$TiO_2$ xerogel (Ni content 75 mol%). Heating rate 2 K/min in synthetic air. The numbers in parenthesis referred to the M/Z values. The dotted lines indicate the temperature at which the IR data shown in Fig. 3 are reported

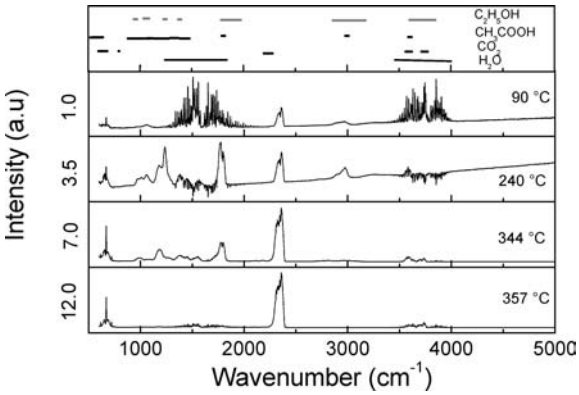


**Fig. 3** Infrared spectra (IR) of a NiO-$TiO_2$ xerogel (Ni content 75 mol%) measured at 90, 240, 344 and 357°C simultaneously with the DTA/TG measurements. Heating rate 2 K/min in synthetic air. The numbers written on the ordinate represent the height of each block. The position of the IR reference peaks of the main components evolved are shown in the top figure [http://webbook.nist.gov/chemistry/]

The most intense mass spectra peaks are those with M/Z = 28 ($C_2H_4^+$ ($C_xH_y$), $CO^+$ (CO, $CO_2$)), M/Z = 32 ($O_2^+$ ($O_2$), M/Z = 14 ($CH_2^+$ ($C_xH_y$), $CO^{2+}$ (CO), $CH_3^+$ ($C_xH_y$)) and M/Z = 16 ($O^+$ ($O_2$, $H_2O$), $CH_4^+$ ($CH_4$), $CH_3^+$ ($C_xH_y$)), M/Z = 43 ($C_3H_7^+$ ($C_xH_y$)). They show a similar behavior and each one appears as a broad single peak with maximum at 344°C but the evolution extends to higher temperatue. Smaller but sharp double peaks are observed with M/Z = 44 ($CO_2^+$ ($CO_2$), $C_2H_5OH^+$ ($C_2H_5OH$), M/Z = 18 ($H_2O^+$ ($H_2O$) and M/Z = 12 ($C^+$ (CO, $CO_2$, $C_xH_y$) resembling the shape of the DTA and GS spectra. These results are in agreement with the evolution of the IR peaks and confirmed that the last DTA peak is mainly related to the formation of oxides.

TG analysis of NiO based sol-gel materials has been only reported with xerogels produced using nickel acetate as precursor where weight losses without indication of the evolved gases were found at about 80°C and between 260 and 300°C [17] and with xerogels made from $NiSO_4$ peptized in acetic acid where the mass loss occurred mostly at about 350°C with the release of $H_2O$, $CO_2$ and organic fragments such as $CH_3^+$, $CH_3CO^+$ [16]. Recently Jesus et al. [34] have studied in detail the thermal decomposition of pure nickel acetate tetra hydrate. The weight loss measured in air at a rate of 30°C/min using TG and MS was found to occur in two steps: a first peak at 120°C, which the authors identified as the evolution of $H_2O$ and acetic acid ($CH_3COOH$), followed by a second single broad peak at 350°C with evolution of $CO_2$, acetone ($CH_3COCH_3$), acetic acid ($CH_3COOH$), ketone ($CH_2CO$) and formic acid (HCOOH) for which the authors suggested a decomposition of the acetate group of a basic compound having the composition $0.56Ni(CH_3COO)_2{\cdot}0.14Ni(OH)_2$ produced during the dehydration of the salt at 120°C and leading to the formation of NiO and Ni.

Ti(Si) xerogel produced from $NiSO_4{\cdot}7H_2O$ peptized by acetic acid also showed a mass loss between 300 and 380°C with evolution of $CO_2$ and $H_2O$. However the whole process was somewhat blurred out due to the cross linking effect of the added silane [23]

## 3.2. Structural properties

### *3.2.1. Thickness and coating appearance of fresh (uncycled) layers*

For layers made with a Ni concentration of 75 mol% and sintered at 300°C, a range of thickness between 20 to 100 nm was achieved by varying the dip-coating withdrawal speed between 0.5 and 4 mm/s respectively. Thicker coating up to 240 nm have been achieved by processing multilayers. All coatings have a slight greenish color. SEM pictures of the coatings made with different Ni molar concentration indicate that all layers are homogeneous without pits or cracks on micrometer scale (not shown).

### *3.2.2. X-ray diffraction and TEM of fresh (uncycled) layers*

X-ray diffraction spectra of NiO-$TiO_2$ layers (Ni concentration of 75 mol%) sintered in air at 250, 300, 400 and 500°C for 30 min are shown in Fig. 4. The layers sintered at 250°C are amorphous and those heat treated at higher temperature exhibit the five peaks of the Bunsenite cubic nickel oxide structure. The crystallinity of the layers increases with the sintering temperature and the crystallite size calculated with the (200) peak are 2.5, 4.7 and 8 nm respectively. A slight (200) preferential orientation is observed. No evidence of a $Ni(OH)_2$, NiOOH and $TiO_2$ crystalline phase is found so that if these compounds exist they are X-ray amorphous.

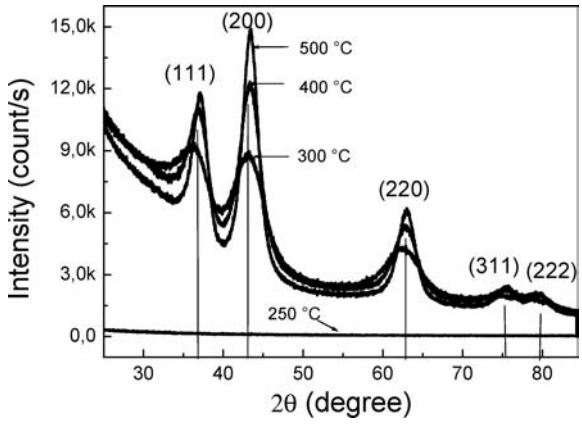


**Fig. 4** XRD patterns for NiO-$TiO_2$ layers (Ni concentration of 75 mol%) deposited on float glass and annealed in air at different temperatures. The vertical lines refer to the Bunsenite nickel oxide phase (PDF-No. 71-1179)

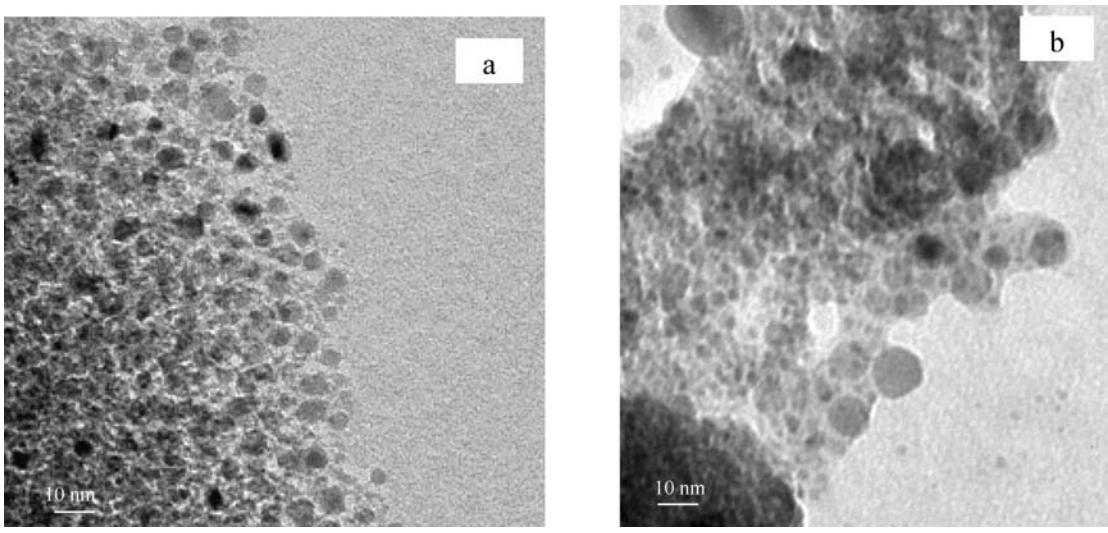


**Fig. 5** TEM pictures of NiO-$TiO_2$ rasped layers (Ni concentration of 75 mol%), deposited on K-glass and sintered at 300°C (a) fresh uncolored layer (b) colored layer after 270 CV cycles

The TEM picture (Fig. 5(a)) of a fresh (uncycled) rasped thin layer shows the presence of many very small round crystalline grains with size of about 8 nm, i.e. about 3 times that of the crystallites, impeded in an amorphous structure.

XRD measurements of layers with Ni concentration between 33 and 90% and sintered at 400°C are shown in Fig. 6. The degree of crystallization increases with the nickel content and the crystallite size calculated with the (111) peak are 3.6, 4.5, 5 and 6 nm for Ni concentration of 33, 66, 87 and 90 mol% respectively. The presence of $TiO_2$ decreases the growth of the NiO crystallites. The crystallite size is smaller than that published for pure NiO films prepared by sputtering, 20–300 nm [28, 35] and sol-gel, 8–150 nm [13, 14]. The width of the peaks is too large to ascertain the formation of a solid solution of $Ti^{4+}$ ions into NiO as observed recently by Wu et al. [36].

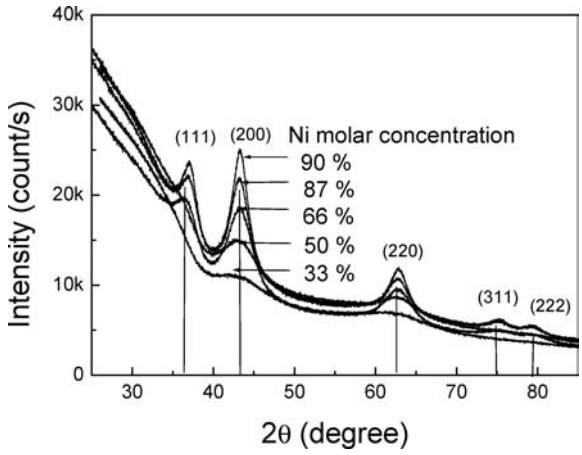


**Fig. 6** XRD pattern for NiO-$TiO_2$ layers of different Ni molar concentration deposited on float glass and sintered at 400°C. The vertical lines refer to the Bunsenite nickel oxide phase (PDF-No. 71-1179)

### *3.2.3. X-ray diffraction and TEM of cycled layers*

As shown below, NiO-$TiO_2$ layers can be deeply brown colored electrochemically. Near grazing incidence (0.3°) of triple layers (240 nm thick) sintered at 300°C and cycled in KOH during 270 cycles exhibited the same Bunsenite NiO cubic structure (Fig. 7). The presence of new peaks containing hydrogen (e.g. $Ni(OH)_2$, NiOOH) was not found in any films. The only differences that are observed is a reduction

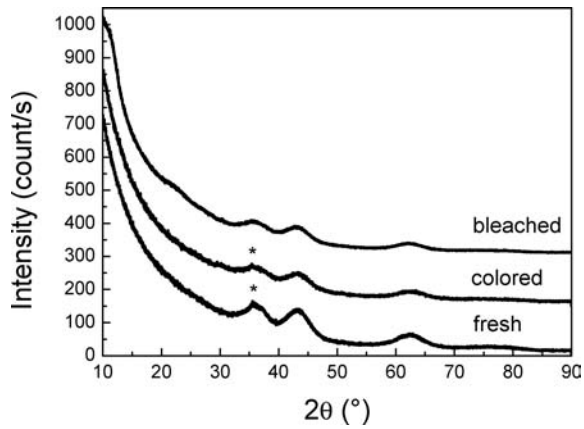


**Fig. 7** Typical XRD pattern of triple NiO-$TiO_2$ layers (Ni molar concentration 75 mol%) as deposited (not cycled), colored and bleached (after 270 CV cycles) deposited on ITO coated glass and sintered at 300°C. The solid lines refer to the Bunsenite peaks (PDF-No 71-1179), the $*$ to the main ITO peaks (PDF-No.44-1087). The spectra have been shifted vertically

of the intensity of the Bunsenite peaks, an indication of a process of progressive amorphization during cycling, and two broad bands in the bleached layer at around 12° and 22.5° that cannot be attributed to any compounds. The results appear at first sight rather surprising but do not preclude that $Ni(OH)_2$ or NiOOH are present in the cycled layers as these compounds can be located on the outermost part of the very small NiO grains (see Fig. 4(a)) and too thin to be detected.

Figure 5(b) shows a TEM picture of a thin rasped layer in the colored state after 270 CV cycles and rather large morphology changes are observed. Although some larger grains (size 10 to 13 nm) are observed, the layer now consists of many smaller particles with size of about 3 nm i.e. the size of the NiO crystallites (2.5 nm), several of them aggregated in a filament shape. This clearly shows that the fresh NiO grains have been disaggregated into their primary crystallites during cycling. This confirms that the colored layers have a more amorphous structure consisting essentially of very small NiO crystallites (see Fig. 7) with probably hydrogenated compounds that cannot be measured by XRD.

### 3.3. Optoelectrochemical characterization

#### *3.3.1. Potential range −0.6 to +0.6 V vs. SCE*

Figure 8 presents typical cyclic voltammograms measured in 1 M KOH during the 2nd, 100th, 400th, and 1000th cycles for a NiO-$TiO_2$ double layer (Ni content of 75 mol%) sintered at 300°C. The potential was cycled between −0.6 and +0.6 V at a scan rate of 10 mV/s. These potentials were chosen to avoid any side reactions such as oxygen or hydrogen evolutions (see also 3.3b). The change of the transmittance measured at 550 nm during the 100th cycle is also shown.

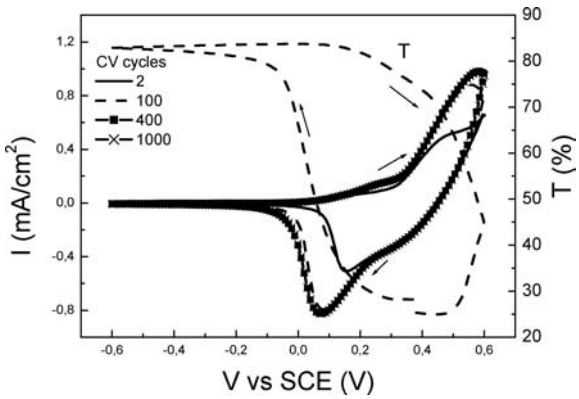


**Fig. 8** Typical CV cycles up to 1000 cycles for a 160 nm thick double NiO-$TiO_2$ layer (Ni concentration of 75 mol%) heated at 300°C, potential range −0.6 to 0.6 V vs. SCE, scan rate 10 mV/s in 1 M KOH. The dotted lines is the variation of the transmittance ($T$) measured during the 100th cycle at $\lambda = 550$ nm

No electrochemical or optical activity are observed in the anodic potential range −0.6 to −0.1 V. Two distinct peaks associated with the coloration of the layer are observed: the first is weak and occurs around 0.25 V while the other at about 0.4 to 0.6 V is strong. They shift to higher potential with the number of cycles up to 300 cycles and then remain stable. In the cathodic range a single intense cathodic peak associated with the layer bleaching is observed at about 0.15 V. It shifts slightly to lower potential value with the number of cycles but remains also stable from 300 cycles. No electrochemical or optical activity is observed for cathodic potential smaller than −0.2 V. The observed shifts of the anodic and cathodic peaks are a clear evidence that the composition of the layer evolved continuously during cycling. The same effect was reported for electrochemically prepared layers [37] and was related to freshly precipitated electronic insulating $Ni(OH)_2$ material during each cycle.

The intensity of the cathodic and anodic peaks increases up to about 300 cycles indicating that the amount of coloring sites available for the redox reaction increases, then remains practically constant up to 1100 cycles and finally starts to decrease (not shown). Such a behavior was also observed for pure sputtered NiO by Avendano [38] who attributed this behavior to the transformation of NiO into $Ni(OH)_2$ while Serebrennikova et al. [39] attributed it to an increased accessibility of Ni(II) sites due to an increased wetting of the layer by the electrolyte. However contrary to our observation (stable current density up to 1100 cycles), pure NiO coatings showed a faster decrease of the electrochemical waves attributed to a degradation of the layer [37].

The charge capacity $Q_c$ has been calculated by integrating the cathodic waves in order to avoid any charge contribution of the oxygen evolution at the positive potential. The value, the number of cycles needed for charge stabilization and the stability of the layer are affected by the parameters of the layer processing (sintering temperature, number of layers, humidity), the scan rate but especially by the thickness of the coating. An example is shown in Fig. 9 for a single layer 80 nm thick and a double layer 160 nm thick both sintered at 300°C . In both cases the cycling life is based on essentially two step process consisting of an *activation period* and a complex *degradation period*. In the first domain the charge density is rather low after the first cycle (5 to 8 mC/cm$^2$) and increases rapidly to reach a broad maximum after 350 cycles for the thin layer and 1000 cycles for the thick layer. The maximum value is higher for the thick layer (20.5 mC/cm$^2$) than that of the thin layer (13.6 mC/cm$^2$). Some tested double layers however presented even a rather large plateau between the 2 periods. In the degradation period the charge density decreases continuously at a slow rate in a complex way. For the double layers system even an abrupt decrease occurs around the 4500th cycles and the charge becomes then very small. Such a behavior was not observed for any of the single

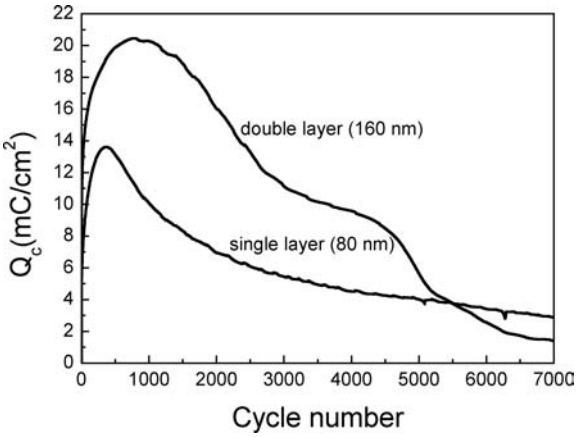


**Fig. 9** Cathodic charge density vs. cycle number for a single (80 nm) and a double (160 nm) NiO-$TiO_2$ layer (Ni concentration of 75 mol%) heated at 300°C calculated from the CV cycles (− 0.6, 0.6 V vs. SCE, scan rate 10 mV/s)in 1 M KOH

layers tested. The fact that both layers show an increase of the charge density during the activation period is compatible with the idea that the EC process occurs intially only in a very thin layer at the interface electrolyte/coating which grows during the activation period to reach eventually the full thickness of the layer when the maximum of $Q_c$ is reached. It is therefore understandable that the maximum and the decrease of $Q_c$ appear earlier for the thin layers than for the thick ones. The ratio of the maximum charge density, 1.5, is smaller than the ratio of the thickness, 2.25. This is an indication that the degradation period initiates probably already in the early stage of the activation period.

The behavior of the optical properties as discussed in detail later is also rather complex and the transmittance change vs. cycle number follows more or less the same behavior, i.e. an increase during the activation period and a decrease during the degradation period.

Pure NiO layers prepared by sol-gel [39], electrochemically [37] and PLD [40] showed a similar behavior with however a more rapid decrease of the charge capacity within 400 cycles only that has been attributed to a degradation of the film during cycling in the electrolyte evolving the transformation of electrochemically active sites into inactive ones with a simultaneous dissolution of the film. However stable charge capacity up to $2 \times 10^4$ cycles has been reported for rf [5] and DC magnetron sputtered hydrated $Ni(OH)_2$ layers [41].

### *3.3.2. Potential range −0.6 to +1 V vs. SCE*

The potentiodynamic range of CV cycles is also a very important factor affecting the charge capacity and hence the electrochromic properties of the layers. Its role was investigated for a 160 nm thick double NiO-$TiO_2$ layer (Ni content of 75 mol%) sintered at 300°C by increasing step by step the positive potential from +0.6 to +1 V while leaving the cathodic potential constant at −0.6 V. Figure 10 shows that ΔOD measured at 550 nm and the charge capacity $Q_c$ are practically linearly related and that both values increase with the positive potential. For +1 V ΔOD reaches a value as high as 0.8 and the coating shows a very dark brown color (Fig. 11) where it is observed that the main effect of the electrochromism takes place in the UV and visible range with a rather weak coloration in the IR range. The shape of the absorbance spectrum (ΔOD) is rather smooth without prounounced peaks. It is interesting to note that the coloration efficiency (CE) corresponding to this coloration change and calculated as $\Delta OD/Q_C$ with $Q_C = 20{,}8$ mC/cm$^2$ is rather high. This is certainly related to the smallness of the NiO grains that have a quite high surface area where the redox reactions and consequently the coloration occur. This is an important result for applications.

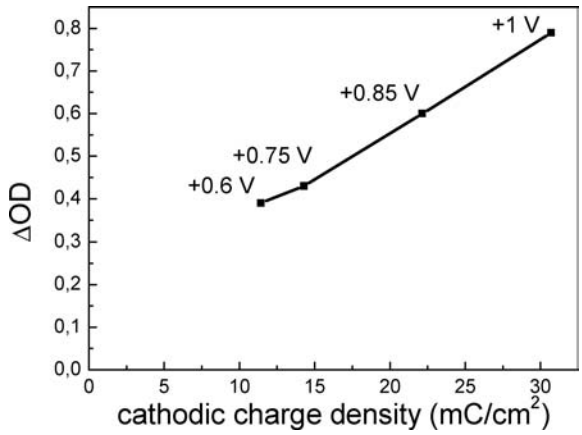


**Fig. 10** Change of optical density, ΔOD at 550 nm versus cathodic charge density for a 160 nm thick NiO-$TiO_2$ double layer heated at 300°C obtained around the 50$^{th}$ CV cycle (activation period) in KOH. The potential scans have been done between −0.6 V vs. SCE and anodic potentials ranging from +0.6 to +1 V vs. SCE at a rate of 10 mV/s

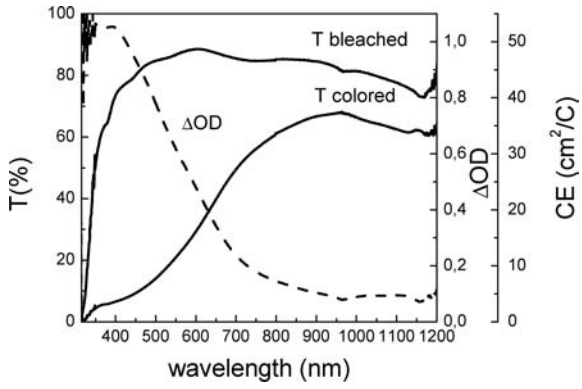


**Fig. 11** Optical transmittance spectra of a 160 nm thick $NiO_2$-$TiO_2$ double layer heated at 300°C measured in the colored and bleached states during the 50$^{th}$ CV cycle. The layer was bleached and colored by a 20 s polarization at −0.6 V and +1 V vs. SCE respectively. ΔOD and the coloration efficiency are also shown

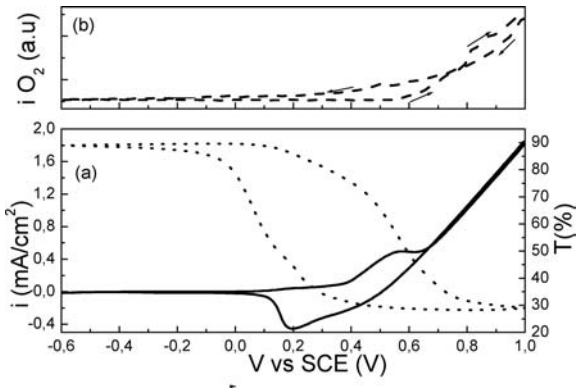


**Fig. 12** 20th CV cycle (−0.6, +1 V vs. SCE) of a 160 nm thick double NiO-$TiO_2$ layer (Ni content 75 mol%), scan rate 10 mV/s in 1M KOH (—) and transmittance change measured at $\lambda = 550$ nm (– –) (b) mass spectrum of the $O_2$ gas, evolved inside the EC cell during the CV cycle

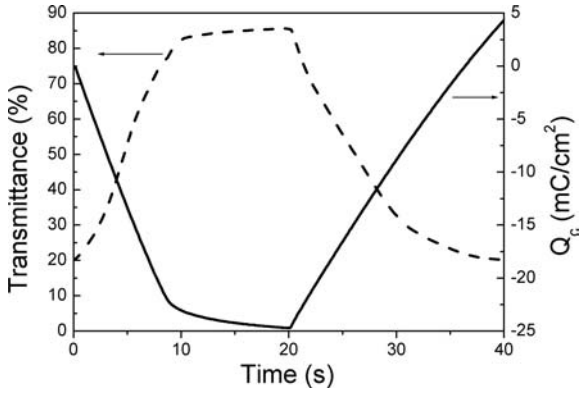


**Fig. 13** Cathodic charge density and transmittance variation measured at 550 nm for a 80 nm thick single NiO-$TiO_2$ layer (Ni content of 75 mol%) in KOH during the 50th CA cycle (−0.6, +0.85 V vs. SCE, 20 s)

A typical transmittance variation of a 80 nm thick layer measured at 550 nm during the 20th CV cycle i.e. during the early part of the activation period (−0.6, +1 V, scan rate 10 mV/s), and the corresponding CV voltammogram are shown in Fig. 12. The anodic and cathodic peaks are similar to those shown in Fig. 8 except that a strong increase in the current density is observed for $V > 0.7$ V. It is accompanied by a very small decrease in transmittance but as shown on the top of the figure, a simultaneous mass spectroscopy determination indicates that this behavior is due to oxygen evolution (also observed as small bubbles) originating from the decomposition according to the reaction: $4OH^- \rightarrow 2H_2O + O_2\,(g) + 4e^-$. No other gases have been detected. As before no electrochemical or optical activities are observed for potential smaller than −0.1 V. The decrease in the transmittance starts in the anodic range at +0.1 V reaching a minimum at +1 V with a maximum slope between 0.45 and 0.7 V. Bleaching starts in the cathodic scan at $V = 0.4$ V reaching again the initial transparent state at −0.4 V with a maximum slope between +0.2 and 0 V.

The overall behavior of the cathodic charge $Q_c$ versus cycle number is similar to that shown in Fig. 9 except that the values of $Q_c$ are higher, that the position of the maxima occurs after a smaller number of cycles and that the rate of degradation period is faster.

The response time of the layer (charge and optical transmittance) is fast and in the range of a few seconds. Figure 13 shows the typical evolution of the charge and transmittance change of an 80 nm thick layer with Ni content of 75 mol% sintered at 300°C during the 5th chronoamperometry (CA) cycle (−0.6, + 0.85 V/20 s).

### *3.3.3. Effect of Ni molar concentration*

The electrochromic activity of sol-gel layers sintered at 300°C made with Ni molar concentration varying between 33% to 100% has been tested in 1 M KOH. The voltamograms have basically the same shape but the maximum of the anodic current density decreases with the increase of Ti content and its position shifts to lower potential while that of the maximum of the cathodic current density shifts to higher positive potentials.

Figure 14 shows the transmittance change up to 700 CV cycles measured at 550 nm with two typical compositions, a pure NiO and a NiO-$TiO_2$ with Ni content of 75 mol% both sintered at 300°C and cycled between −0.6 and +75 V. For pure NiO the transmittance of the colored state decreases from 50% to a minimum of 10% in about 50 CV cycles and remains then constant while the transmittance of the bleached state remains practically constant ($T = 85\%$) during the first 50 cycles and then decreases sharply but continuously. The pure layer becomes therefore permanently colored already after 50 cycles. On the contrary for the NiO-$TiO_2$ layer the

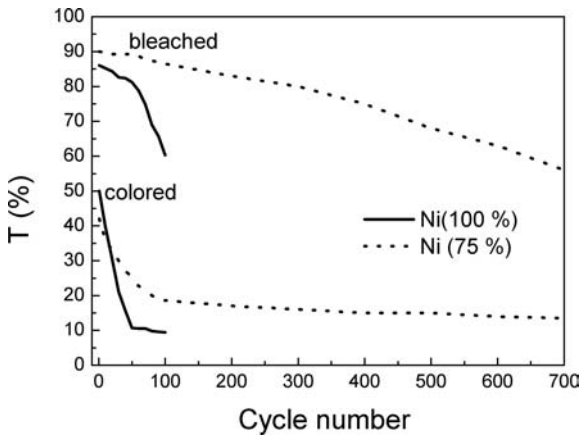


**Fig. 14** Transmittance of the bleached and colored states measured at 550 nm during 100 CV cycles (0.6, +75 V vs. SCE/10 mV/s) in 1 M KOH for a 75 nm thick pure single NiO layer heat treated at 300°C for 30 min (–) and a 80 nm thick NiO-$TiO_2$ layer with Ni content of 75 mol%, cycled between the same potentials. up to 700 cycles (—)

transmittance in the bleached state decreases only slightly but continuously and that of the colored state decreases from 43% down to a minimum of 12%. The decrease of the transmittance in the colored state is compatible with the results shown in Fig. 9 and corresponds to the increase of the charge density observed during the activation period.

The NiO-$TiO_2$ layers becomes therefore also permanently colored, but not as fast as pure NiO and the effect became more pronounced in the degradation period. The initial value of the transmittance in the bleached state ($T = 90\%$) can be however fully recovered if the negative potential of $-0.6$ V is applied for a long time ($>1$ h) or if a more negative potential e.g. $-1.5$ V is applied for a few minutes only. However by further cycling the layer in the normal condition ($-0.6$ to $+0.6$ or $+1$ V) the permanent coloration is fully recovered. Therefore the degradation period is associated with the formation in the layer of passive colored sites that probably are initially formed in a surface layer that grows with cycling through the whole layer. Moreover the formation of these passive sites leads to an extreme fragility of the layer that self-disaggregate slowly (dissolution) into the electrolyte, where tiny colored floating spots can be clearly observed by the eye. This process continues till the layer is fully removed from the substrate, a phenomenon that is observed after more than 7000 cycles (see Fig. 9).

Figure 15 shows finally a summary of the results for NiO-$TiO_2$ layer with Ni molar concentrations varying between 33 to 100%. The permanent coloration in the bleached state is clearly depending on the Ni concentration and becomes quite high for values higher than 80 mol%. The transmittance of the colored state and consequently the values of $\Delta$OD after 100 cycles are also strongly dependent on the NiO content. Comparing the values of $T_{\text{bleached}}$, $T_{\text{colored}}$ and $\Delta$OD after 100 CV cycles (i.e. typically near the end of the activation period), pure NiO layers are therefore not suitable for EC devices. Although they show the highest change in optical density (Fig. 15) they lose very fast their transparency in the bleached state after cycling. They are also easily removed by rubbing with a finger and have therefore a poor adhesion to the substrate. Those with high content of Ti are also not adequate as the electrochromic effect is poor. They are also very sensitive to humidity and tend to form a white $Ti(OH)_2$ layer on their surface. The layers with the best compromise are those having a Ni content around 75 to 80 mol%. In the activation period they remain practically transparent in the bleached state and present a rather high variation of the optical density, typically 0.65, i.e. 80% of that of the pure NiO layer. Moreover, for this composition, a better adhesion to the substrate and a better stability are observed.

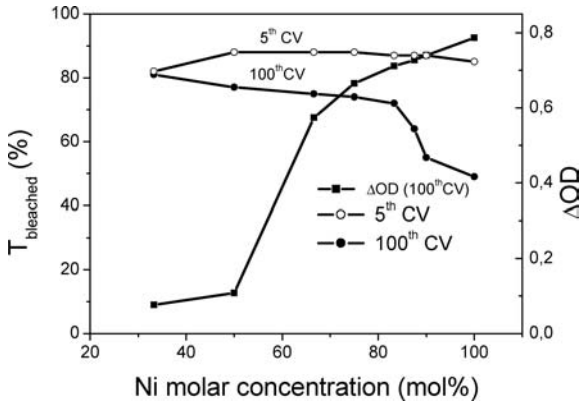


**Fig. 15** Change of the transmittance of the bleached state and optical density measured at 550 nm for single NiO-$TiO_2$ layers with different Ni molar concentration, sintered at 300°C for 30 min

Martini et al. [20] also found that the change in optical density decreases by increasing the Ti content up to a ratio of Ni molar concentration of 54% followed by an unexpected increase for higher Ti content. Such a behavior is not found here and the optical density always decreases by increasing the Ti content (Fig. 15).

### *3.3.4. Effect of heat treatment*

Dip-coated layers (75 mol% Ni content) were heated for 30 min at different temperatures ranging from 250 to 500°C and then cycled in 1M KOH electrolyte. Figure 16(a) shows typical CV curves measured during the 50$^{\text{th}}$ CV ($-0.6$, $+0.6$ V, scan rate 10 mV/s). The overall behavior of the current density is similar but the large decrease of the maximum value and a shift of its position is observed especially for sintering temperatures $T \geq 350$°C. The change in optical density of the layers measured during the 1$^{\text{st}}$ and the 100$^{\text{th}}$ cycles (activation period) is shown in Fig. 16(b). The $\Delta$OD values increase during the activation period for all sintering temperatures but reach a constant high value only for layers sintered up to 300°C. The lower value obtained for the layers sintered at $T \geq 350$°C may be due to the better dehydration of the layers indicating that the water content and the hydration of the surface is an important factor to get a high electrochromic activity [3], or to the presence of larger crystalline particle size which agglomerated in a more compact morphology resulting in lower ionic conductivity. Although the layers heated at 250°C and 300°C showed a large change of the optical density, they gain a slight permanent coloration by cycling. On the contrary the layer sintered at 350°C shows the same change in optical density but its transmittance change in the bleached state remains unaltered by cycling ($T = 89\%$) and is therefore the best compromise.

### *3.3.5. Effect of thickness*

Single NiO-$TiO_2$ layers have been deposited on *K*-glass by dip coating at different withdrawal speeds ranging from 1 to

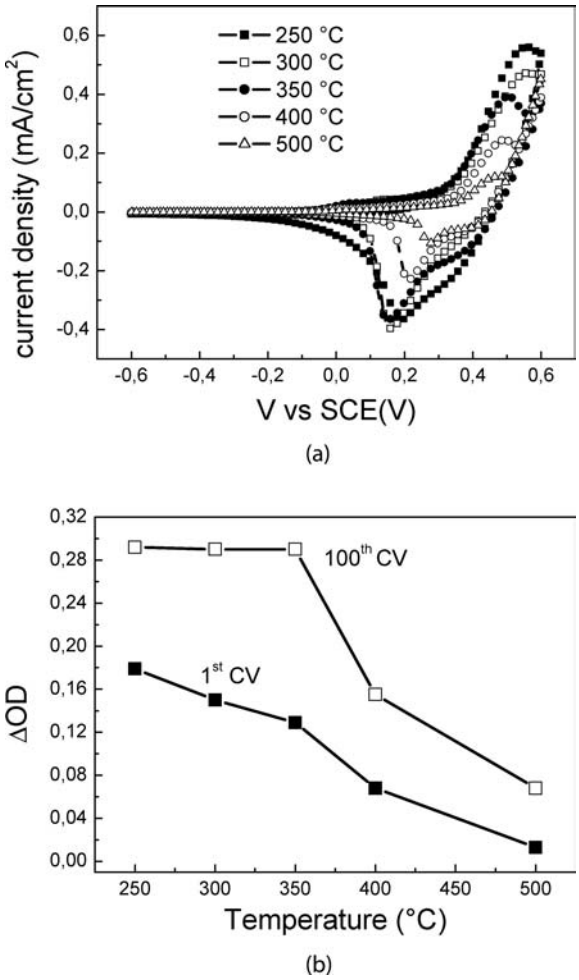


**Fig. 16** 50th voltammogram (− 0.6 to + 0,6 V vs. SCE, scan rate 10 mV/s) in 1M KOH of 80 nm thick NiO-$TiO_2$ single layers (Ni content 75%) heat treated at different temperatures, (b) corresponding change of the optical density measured at the wavelength of 550 nm during the 1st and 100th CV cycles

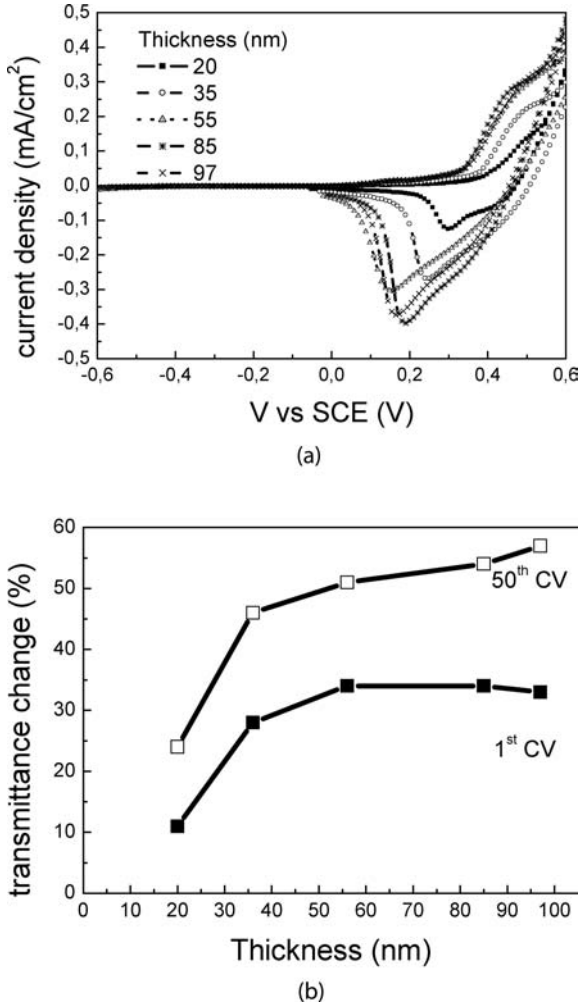


**Fig. 17** (a) 1st CV cycle (−0.6,1 V vs. SCE/10 mV/s) in 1 M KOH for single NiO-$TiO_2$ layers of different thicknesses sintered at 300°C (b) transmittance change during the 1st and 50th CV cycles, vs. thickness

4 mm/s to get different thicknesses. They have been sintered at 300°C and tested in KOH as described before. Figure 17(a) shows that the shape of the first CV cycle changes with the thickness of the layer. The current and consequently the charge increase up to about 55 nm and then remain constant. The transmittance change $\Delta T$ follows a similar behavior (Fig. 17(b)). When measured during the 50th CV cycle i.e. in the early part of the activation period the same overall behavior is observed but with higher values of the current, inserted charge and transmission change (see also Fig. 9) and a saturation effect is also observed for thicknesses higher than 60 nm. This result is also a clear evidence that in the activation period the coloration of the layer is initially limited to a thin surface layer only that grows with cycling.

Another confirmation of this observation was obtained by performing the following experiment: an 80 nm thick single NiO-$TiO_2$ layer was colored during 50 cycles. The colored material was found to be easily removed with a cotton stick, leaving behind an intact transparent layer and the step left measured with a profilometer was 56 nm. Tests made during further cycling showed that the rest of the layer could be colored again. Similar tests made with layers cycled till reaching the end of the activation period (and of course also during the degradation period) show that now the whole thickness of the layer was easily removed by rubbing indicating that the coloring region had grown through the full thickness of the layer.

It is therefore proved that during the initial cycles of the the activation period there is the formation of a thin layer where the EC process takes place. As shown in a subsequent paper where Quartz Crystal Microbalance experiments measured during the 2 periods are reported [42], a gradual change of the composition of the surface layer occurs due to the interacalation/deintercalation of $OH^-$ and $H^+$ species and drastic variations occur in the degradation period. The fact that the colored surface layer is mechanically very soft compared to

an uncolored layer is due to the intercalation/deintercalation of $OH^-$ and $H^+$ species that modify the morphology of the layer and introduce considerable tensile stress (already reported for rf sputtered NiO layer [39]) that eventually leads to a gradual dissolution of this surface layer into the electrolyte.

### *3.3.6. Final discussion*

Electrochromism in NiO-based films is rather complicated and the nature of the electrochemically active phases remains largely debated. The published results are difficult to be compared as the EC properties depend largely on the crystallinity, the stoichiometry, the morphology and the texture of the layers. Nevertheless it can be stated whatever the layer production process is, that the reversible transition from a bleached to a colored state is related to a charge-transfer process between a Ni (II) compound and a Ni (III) ones and that all layers suffered a degradation process when cycled in a KOH-based electrolyte in competition with the electrochemical process. The newly developed NiO-$TiO_2$ sol-gel layers behave in a similar way. This paper has shown nevertheless that layers made with 75 mol% Ni concentration and sintered between 300 and 350°C are better than pure NiO ones. In the as deposited state they are highly homogeneous whatever the thickness is, contrary e.g. to those prepared by PLD recently reported by the group of Tarascon [40, 43] and consist of very small crystalline particles of NiO with size of ∼9 nm and crystallite size ∼2.5 nm dispersed in an X-ray amorphous $TiO_2$ network. A solid solution Ni-Ti-O cannot be discarded but could not be ascertained.

The following mechanism can be proposed to explain the electrochromic results. The immersion of a NiO-$TiO_2$ layer into the aqueous KOH electrolyte leads to the rapid formation of a hydrated thin layer probably not thicker than 40 nm, i.e. smaller than the thickness of the used layers with the formation of amorphous $Ni(OH)_2$ sites. These sites have not been observed by XRD or TEM and are certainly very small. As cycling is initiated, electrochemical reactions based on a Faradic process occurs corresponding to the oxidation of the hydroxide sites into oxyhydroxide sites ($\beta$(III) NiOOH). The reactions follow certainly the classical Bode process $Ni(OH)_2 + OH^- \rightarrow Ni\,OOH + H_2O + e^-$ leading to a brown color. These phases are amorphous as they have not been observed by X-ray diffraction (Fig. 7). The formation of this very thin layer explains the low amount of cathodic charge (Fig. 9) and the small transmission change observed during the initial cycles (Fig. 14). By increasing the cycle number, the thickness of the thin layer that involves the $Ni(OH)_2$ phase in the bleached state and the NiOOH phase in the colored state increases to eventually involves the total thickness of the layer. In addition to this process a slow rate degradation process of the oxidized phase begins to be superimposed.

This process is responsible to the slow down of the growth of $\Delta Q_c$ and $\Delta$OD so that these values reach a broad maximum value, higher for thick layers than thin ones, and occurring after about 350 cycles for an 80 nm single layer and about 1000 cycles for 180 nm thick double layers (Fig. 9).

Before reaching these maxima the morphology of the layers has continuously changed and consists essentially of smaller NiO grains, the size of the crystallites (about 2.5 nm) that are loosely imbedded in the amorphous $TiO_2$ network so that the layers become soft and easily rubbed both in the bleached or the colored state. Passing the steady state, the degradation period proceeds in which $\Delta Q$, $\Delta T$ and $\Delta$OD slowly decrease toward zero values in a rather complex way.

The permanent coloration of the bleached state initiates already in the early cycles (see Fig. 14) and becomes more important with further cycling. The bleached state can be however fully recovered by applying either a −0.6 V vs. SCE potential for about 1 h or a more negative potential (e.g. −1.5 V) during a few minutes. Nevertheless the permanent coloration is fully recovered if the next cycles are performed between −0.6 V to +0.6 V or +1 V. This indicates that a permanent passive phase that cannot be reduced in the normal conditions is growing. This stable colored phase seems to occur at the surface region and confers to the layer an extreme fragility since even tiny colored spots floating in the electrolyte can be clearly observed by the eye. Therefore the active EC layer becomes thinner and thinner till its complete removal after about 7000 to 10000 cycles.

Our results are therefore in agreement with the accepted set of redox reactions proposed by Bode [30]. However they cannot yet ascertain the exact nature of the passive layer. In a forthcoming paper it will be shown that the degradation period is associated with an unusual large increase of the mass of the layer after each cycle due to the irreversible incorporation of $OH^-$ groups and/or the irreversible formation of water ($OH^- + H^+ \rightarrow H_2O$).

## 4. Conclusion

NiO-$TiO_2$ xerogels and layers have been prepared with different Ni molar concentration by the sol-gel route. Thermal analysis of xerogels has been performed using simultaneous DTA-TG coupled to mass and infrared spectroscopy. Single and multiple layers with total thickness up to 240 nm have been deposited on FTO-coated glass by dip-coating and sintered up to 500°C. They were transparent and exhibited a NiO bunsenite structure regardless of the Ni concentration. Their electrochromic properties have been tested using cyclic voltammetry and chronoamperometer in 1 M aqueous solution of KOH as a function of the potential range, Ni content, heat treatment and thickness. Pure NiO layers showed a poor adhesion on the substrates, a rather high permanent

brown coloration after already 50 CV cycles and were easily degraded in the electrolyte. The adhesion was clearly improved by increasing the Ti content. Up to 400 cycles the transmission in the bleached state remains high and constant (>75%) when the Ni molar concentration is <85% but both the optical density and the charge capacity decrease continuously by increasing the Ti content. The layers that present the best properties are 160 nm thick double layer having a Ni molar concentration of 75% and sintered between 300 and 350°C. When cycled between −0.6 and + 1 V they showed a deep reversible brown coloration between 90 and 20% (at 550 nm), a much better stability than the pure NiO layers and a fast switching time <I0 s. The EC process was divided into 2 periods. The coloration of NiO-$TiO_2$ initiates in thin interface layers (about 40–50 nm) that grows with cycling till reaching the full depth of the layer at the end of the activation period. This lasts up to about 1000 cycles depending on the potential range and the thickness of the layer. Practically simultaneously a slow degradation period takes place in which a passive, irreversible colored and very fragile layer is formed. This period is clearly observed after about 1000 cycles in which both the exchanged charge and the transmission in the bleached state and correspondingly the change in optical density, decrease. Due to the extreme fragility of this passive layer, the NiO-$TiO_2$ is also gradually disaggregated into the electrolyte till the layer is completely removed from the substrate after about 7000 to 10000 cycles. These observations are in agreement with the accepted Bode model but the exact nature of the different phases could not be yet ascertained with precision.

**Acknowledgment** The authors thank Dr. I. Grobelsek (INM) for X-ray diffraction measurements and Mrs A. Haettich (INM) for the SEM and TEM investigations, the state of Saarland and Federal Ministry for Research and Education (Germany) for the financial support. One of the authors (A. Al-Kahlout) would like to thank Al-Azher university (Gaza) for the partial financial support.

## References

1. Avendano E, Azens A, Niklasson GA, Granqvist CG (2004) Solar Energy Materials and Solar Cells 84:337
2. Granqvist CG (1995) Handbook of inorganic electrochromic materials. Elsevier, The Netherlands
3. Fantini MCA, Bezerra GH, Carvalho CRC, Gorenstein A (1991) SPIE Optical Material Technology for Energy Efficiency and Solar Energy Conversion 1:1536
4. Passerini S, Scrasati B, Gorenstein A, Andersson AM Granqvist CG (1989) J Electrochem Soc 136:3394
5. Svensson JSEM, Granqvist CG (1986) Applied Physics Letters 49:1566
6. Gorenstein A, Decker E, Fantini M, Estrada W (1990) SPIE Institutes for Advanced Optical Technologies IS-4:272
7. Estrada W, Andersson AM, Granqvist CG (1988) Journal of Applied Physics 64:3678
8. Bouessay I, Rougier A, Beaudion B, Leriche JB (2002) Applied Physics 186:4901
9. Agrawal A, Habibi HR, Agrawal RK, Cronin JP, Robert DM, Caron-Popowich RS, Lampert CM (1992) Thin Solid Films 221:239
10. Morisaki S, Kawakami K, Baba N (1988) Japanese Journal of Applied Physics Part I 27:314
11. Ezhof BB, Malandin OG (1991) Journal of the Electrochemical Society 138:885
12. Maruyama T, Arai S (1993) Solar Energy materials and Solar Cells 30:257
13. Surca A, Orel B, Pihlar B, Bukovec P (1996) Journal of Electroanalytical Chemistry 408:83
14. Sharma PK, Fantini MCA, Gorenstein A (1998) Solid State Ionic, Diffusion & Reaction 457:113
15. Surca A, Orel B, Pihlar B (1997) Journal of Sol-Gel Science and Technology 8:743
16. Korosec RC, Bukovec P, Pihlar B, Surca A, Orel B, Drazic G, Solid State Ionic 165:191
17. Korosec RC, Bukovec P (2004) Thermochimica Act 410:65
18. Garcia-Miquel JL, Zhang Q, Allen SJ, Rougier A, Blyr A, Davies HO, Jones AC, Leedham TJ, Williams PA, Impey SA (2003) Thin Solid Films 424:165
19. Lopez DS (2003) Diploma Thesis, Leibniz-Institut für Neue Materialien, Saarbruecken, Germany
20. Martini M, Brito GES, Fantini MCA, Craievich AF, Gorenstein A (2001) Electrochemica Acta 46:2275
21. Moser FH, Lyman NR, Method for deposition of electrochromic layers. United States Patent, Appl. No. 016663
22. Park J-Y, Ahn K-S, Nah Y-C, Shim H-S (2004) Journal of Sol-Gel Science and Technology 31:323
23. Surca A, Orel B, Cerc-Korosec R, Bukovec P, Pihlar B, Journal of Electroanalytical Chemistry 443:57
24. Svegel F, Orel B, Kaucic V (2000) Solar Energy 86:523
25. Lambert CM, Omstead TR, Yu PC (1986) Proc Soc Photo-Opt Instrum Eng 562:16
26. Carpenter MK, Conell RS, Corrigan DA (1987) Sol Energy Mater 16:333
27. Nagai J (1993) Solar Energy Materials and Solar Cells 31:291
28. Azens A, Kullman L, Vaivars G, Nordborg H, Granqvist CG (1998) Solid State Ionic 113–115:449–456
29. Passerini S, Scrosati B (1994) J Electrochem Soc 141:1025
30. Bode H, Dehmelt K, Witte J (1966) Electrochimica Acta 11: 1079
31. Baudry P, Rodrigues ACM, Aegerter MA (1990) Journal of Non-Crystalline Solids 121:319
32. Bhargava R, Levin W (2004) Applied Spectroscopy 58:995
33. Nam K-W, Kim K-B (2002) Journal of Electrochem Soc 149: A364
34. De Jesus JC, Gonzalez I, Quevedo A, Puerta T (2005) Journal of Molecular Catalyst A Chemical 228:283
35. Ferreiraa FF, Tabacniksa MH, Fantini MCA, Fariab IC, Gorenstein A (1996) Solid State Ionics 86–88:971
36. Wu Y, He Y, Chen T, Weng W, Wan H (2005) Materials Letters 59:3106
37. Fantini M, Gorenstein A (1987) Solar Energy Materials 16:487
38. Avendano E (2004) Electrochromism in Nickel-based oxides, Thesis, University of Uppsala, Finland
39. Serebrennikova I, Birss VI (1997) Journal of Electrochem Soc 144, 566
40. Bouessay I, Rougier A, Poizot P, Moscovici J, Michalowicz A, Tarascon J-M (2005) Electrochemica Acta 50: 3737
41. Scarminio J, Estrada W, Andersson A, Gorenstein A, Decker F (1992) J Electrochem Soc 139:1236
42. Al-kahlout A, Aegerter MA, submitted
43. Bouessay I, Rougier A, Tarascon J-M (2004) J Electrochem Soc 151:H145